

Nanocomposites of sodium alginate biopolymer and CdTe/ZnS quantum dots for fluorescent determination of amantadine

Ghasem Rezanejade Bardajee¹ · Zari Hooshyar¹ · Rouhollah Soleyman²

Received: 17 December 2016 / Accepted: 28 April 2017 / Published online: 24 July 2017
© Springer Science+Business Media Dordrecht 2017

Abstract A type of novel nanocomposite was successfully synthesized by embedding glutathione capped CdTe/ZnS QDs into sodium alginate biopolymer. The prepared nanocomposite was characterized using transmission electron microscopy (TEM), thermogravimetric analysis (TGA), and Fourier transform infrared (FT-IR), fluorescence, and UV–vis spectroscopy. When the obtained nanocomposite interacted with amantadine, its fluorescence intensity was effectively quenched. Under the optimized conditions, the as-prepared nanocomposite provided an efficient platform for detection of amantadine drug within a linear range of $3.1\text{--}27.9 \times 10^{-6}$ mol/L with a detection limit of 0.09×10^{-6} mol/L. Because of the satisfactory results for amantadine determination in real samples, it is confirmed that the synthesized nanocomposite is attractive and reliable for use in biological detection and related fields.

Keywords Nanocomposite · Amantadine determination · Polysaccharide

Introduction

In recent years, fluorescent nanosensors have attracted great attention in a diverse range of biological applications such as cell labeling, genomic detection, and optical sensors [1–3].

Many of the fluorescent nanosensors were made based on fluorescence quenching (as signal output) of the fluorophore in the presence of the analyte, and it was restored upon binding with the target analyte that competes with the fluorescent nanosensors [4, 5]. Compared with other techniques, these nanosensors offered advantages such as their ease and speed of use and their sensitivities [2, 3]. They could be made using nanomaterials such as nanoparticles, multiwalled carbon nanotubes, carbon nanofibers, polyaniline nanofibers, graphene nanosheets, and their nanocomposites [6–14].

Nanocomposites consist of a bulk matrix with nano-dimensional material dispersed in bulk matrix [13]. These may have different properties due to markedly different structure and chemistry of the nanocomposite from that of the component materials [14]. Quantum dots (QDs) can be dispersed in polymers to make nanocomposites, and they doubtless present a scientific revolution for the twenty-first century [15].

QDs, with sizes in the range 2–10 nm, possess some unique optical properties, including high-emission quantum yields, broad absorption peaks, narrow and symmetric emission peaks, and good chemical and optical stabilities [16–20]. These properties are strongly dependent on the radiative and non-radiative processes of excited QDs, which are sensitive to the nature of surface states and the chemical/physical environment [17, 19]. Hence, much progress in controlled synthesis of high quality QDs, as well as the effective surface modifications, are used to fabricate devices with excellent optical characteristics and desired surface binding sites [15, 17, 19]. Morphologically, the trap sites on the surface of QDs dramatically decrease their fluorescence quantum yields. However, these trap sites can be eliminated after modification of QDs with functional groups and subsequently enhance the optical properties of the QDs [13, 15, 19]. Therefore, capping reagents play an important

✉ Ghasem Rezanejade Bardajee
rezanejad@pnu.ac.ir

¹ Department of Chemistry, Payame Noor University, PO BOX 19395–3697, Tehran, Iran

² Polymer Science and Technology Division, Research Institute of Petroleum Industry (RIPI), Tehran, Iran

role in highly fluorescent QDs. Some researchers used glutathione (GSH) as a capping agent for synthesis of CdTe QDs with high photoluminescence quantum yield in the aqueous phase [21, 22]. GSH, a naturally occurring and readily available tripeptide, was an important water-phase antioxidant and essential cofactor for antioxidant enzymes [23]. Because GSH has many functional groups (e.g. thiols, carboxyl, and amino groups), GSH-capped CdTe QDs show improved water-stability and biological compatibility than other water-soluble QDs [23, 24]. However, the fluorescence intensities of the GSH-stabilized CdTe QDs are weak due to their dissociation by irradiation of excitation light [25, 26]. To overcome this disadvantage, much interest in synthesized CdTe QDs focuses on aqueous CdTe/ZnS QDs with core-shell structure [27, 28]. The growth of inorganic ZnS shell on the surface of CdTe core QDs enhanced fluorescence intensity of QDs and evidently suppressed the toxicity of the QDs themselves in biological environments [29]. Based on the above, the GSH-stabilized CdTe/ZnS QDs have been successfully synthesized by some aqueous methods [30, 31]. Nonetheless, there are still some concerns with how to prepare GSH-stabilized CdTe/ZnS QDs with high stability, sensitivity, and selectivity analysis. Previously, we demonstrated a strong fluorescence activation effect and stability after incorporating QDs into multidentate biocompatible polysaccharides [32–36].

Herein, we used sodium alginate (SA) biopolymer and GSH-stabilized CdTe/ZnS QDs (GSH-CdTe/ZnS QDs) for preparation of a nanocomposite, which has not previously been reported. SA is a polyelectrolyte biopolymer and biodegradable block copolymer [37]. It is extracted from brown seaweeds with an anionic copolymer consisting of 1–4 linked α -L-guluronic (G) and β -D-mannuronic (M) acid residue [38]. It has many functional groups on its chains for electrostatic interaction and coordination sites [37, 38]. As illustrated in Scheme 1, this natural polysaccharide has many functional groups on its chains for electrostatic interaction and

coordination sites of QDs. The obtained nanocomposite was characterized using transmission electron microscopy (TEM), thermogravimetric analysis (TGA), and Fourier transform infrared (FT-IR), fluorescence, and UV–vis spectroscopy. In addition, we also investigated the interactions between the as-prepared nanocomposite and amantadine at different conditions. As a result, the fluorescence quenching of synthesized nanocomposite occurred at 576 nm in the presence of amantadine. The mechanism of the proposed reaction was also investigated. We also used the synthesized nanocomposite to determination of amantadine in its commercial samples. According to the properties of the interactions, we suggest that obtained nanocomposite could be used as a convenient, sensitive, and selective fluorescent nanosensor for amantadine detection.

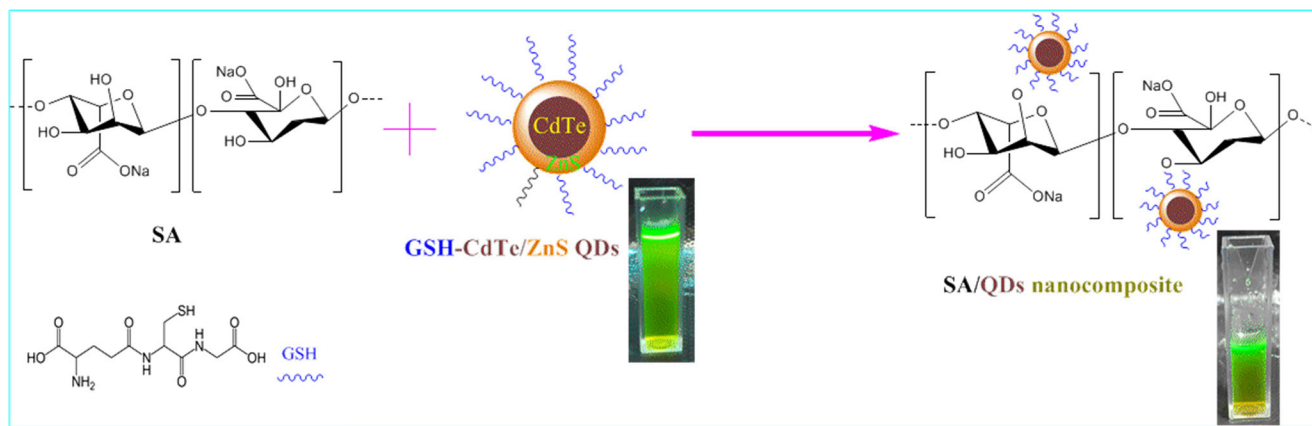
Experimental

Chemicals

Analytical grade chemicals without further purification were used during our work. Sodium alginate (SA), thioglycolic acid, cadmium chloride ($\text{CdCl}_2 \cdot 5\text{H}_2\text{O}$), tellurium powder (Te), sodium borohydride (NaBH_4), and amantadine were obtained from Sigma Aldrich. In addition, Tris (hydroxymethyl) aminomethane (Tris) and glutathione (GSH) were purchased from Acros Organics. Double distilled water was used for preparing solutions.

Apparatus

FT-IR spectra were obtained in a Jasco 4200 FT-IR spectrophotometer. Transmission electron microscopy (TEM) images of the QDs were taken using a Zeiss TEM at an acceleration voltage of 80 kV. Thermogravimetric analysis (TGA) was performed on a TA instrument 2050



Scheme 1 Schematic illustration for preparation of SA/QDs nanocomposite

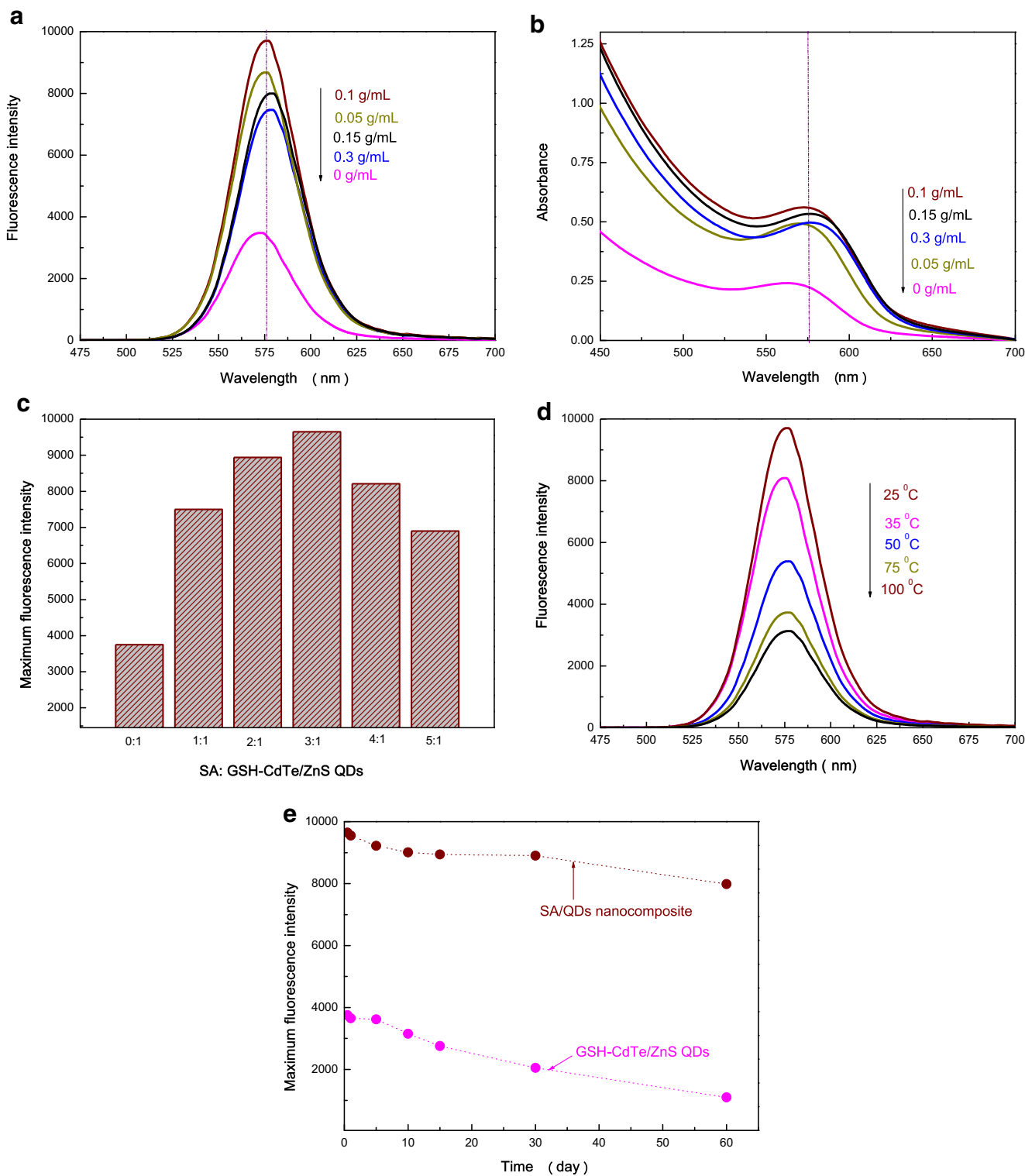


Fig. 1 (a) and (b) fluorescence and absorption spectra of the SA/QDs nanocomposite prepared with different concentration of SA (0, 0.05, 0.1, 0.15, and 0.3 g/mL), (c) effect of SA:GSH-CdTe/ZnS QDs ratio on the fluorescence intensity of the SA/QDs nanocomposite, (d) effect of

reaction temperature on the fluorescence intensity of the SA/QDs nanocomposite, and (e) effect of aging on the fluorescence properties of the SA/QDs nanocomposite and GSH-CdTe/ZnS QDs

thermogravimetric (TG) analyzer under N₂ atmosphere (25 mL/min) at a scan rate of 20 °C/min. The absorbent and fluorescent investigations were carried out using

Shimadzu UV-visible 1650 PC spectrophotometer and SCINCO's Fluorescence Spectrometer FluoroMate FS-2, respectively.

Synthesis of GSH-CdTe/ZnS QDs

GSH-CdTe/ZnS QDs preparation was performed as described in the literature with some modifications [30, 31]. This method had three steps. In the first step, colorless solution of NaHTe was prepared. A 0.025 g sample of Te powder was dissolved in 0.025 g of NaBH₄ in a flask containing 2.5 mL of water and kept under vigorous stirring and argon bubbling for 2 h. In the second step, an aqueous solution of NaHTe, CdCl₂ · 5H₂O, and thioglycolic acid with molar ratio fixed at 1:0.5:2.4 was prepared. By using concentrated NaOH solution, the pH was adjusted to 8–9 and the resulting solution was refluxed at 100 °C for 1 h under argon to form thioglycolic acid-CdTe QDs. In the third step, 0.0136 g ZnCl₂ and 0.1229 g GSH were dissolved in 1 mL water while the pH of solution was adjusted to 8. This solution was added to the as-prepared thioglycolic acid-CdTe QDs solution and refluxed for another 2 h.

Synthesis of SA/QDs nanocomposite

The synthetic process of the SA/QDs nanocomposite is shown in Scheme 1. At first, in order to optimize the concentrations of SA, different concentrations of SA (0.05, 0.1, 0.15, and 0.3 g/mL) were dissolved in 25 mL of double distilled water and stirred to make a homogeneous solution. After 30 min, 5 mL of the obtained GSH-CdTe/ZnS QDs was added to a round bottom flask containing prepared SA solution. The solution was mixed at room temperature for 1 h.

To optimize the ratio of SA:GSH-CdTe/ZnS QDs, 0.1 g/mL of SA was dissolved in 25 mL of double distilled water and stirred for 30 min. Then to make a 1:1 ratio of SA:GSH-CdTe/ZnS QDs, 5 mL of GSH-CdTe/ZnS QDs was mixed with 5 mL of SA solution. To make a 2:1 ratio of SA:GSH-CdTe/ZnS QDs, 5 mL of GSH-CdTe/ZnS QDs was mixed with 10 mL of SA solution. The same method was used for preparation of different ratios of SA:GSH-CdTe/ZnS QDs. After that the solution was mixed at room temperature for 1 h.

To optimize the temperature, 0.1 g/mL of SA was dissolved in 25 mL of double distilled water and stirred for 30 min. Then, 5 mL of obtained GSH-CdTe/ZnS QDs was added to a round bottom flask containing prepared SA solution. The solution was mixed at different temperatures (25, 35, 50, 75, and 100 °C) for 1 h.

Analytical procedure

Amantadine stock solution (0.63 mmol/L) was prepared with Tris-HCl buffer solution (0.10 mol/L, pH 7.40). Two milliliters of solution with an appropriate amount of amantadine, SA/QDs nanocomposite solution, and Tris-HCl solution were prepared and mixed thoroughly by gentle shaking. Five minutes later,

the fluorescence spectra were recorded in the 490–800 nm emission wavelength range with the excitation of 475 nm.

Results and discussions

Optimization of the SA/QDs nanocomposite reaction

The fluorescence spectra of the SA/QDs nanocomposite were prepared with different concentrations of SA. As can be seen from Fig. 1a, the fluorescence intensity of the SA/QDs nanocomposite was increased gradually with the increasing concentration of SA from 0 to 0.1 g/mL, which may be attributed to the passivation of QDs via hydroxyl and carboxyl functional groups of SA polysaccharide [35]. This passivation can be confirmed by comparing FT-IR spectra of the SA/QDs nanocomposite with FT-IR spectra of SA biopolymer as described next. However, further passivation of the QDs surface by these groups occur as the SA concentration increases. Therefore, the fluorescence intensity of the SA/QDs nanocomposite decrease due to the decrease in surface trap sites, increase in the intensity of bandgap emission, and decrease in surface trap emission. A further increase of the SA concentration (from 0.1 to 0.3 g/mL) caused an obvious decrease of the fluorescence intensity because the effective movement of the QDs was hindered by the increase in viscosity of the medium [34]. In addition, fluorescence spectra of all samples had a symmetric and narrow FWHM, which proved that the QDs were nearly monodisperse and homogeneous in the SA/QDs nanocomposite. Nevertheless, the fluorescence peaks of samples were clearly shifted. It was assumed that the shifting of fluorescence peaks at a lower value may be due to the presence of ligand exchange processes in the interaction between SA and QDs. Therefore, the SA biopolymers were replaced with GSH ligands and made an etching of the surface of the QDs. To explore further, the absorption spectra of all aforementioned samples were investigated (Fig. 1b). It was observed that the all samples showed strong excitonic absorptions at different wavelength. The phenomenon might be attributed to obtain smaller/larger particles of QDs in reaction [31]. The average sizes of SA/QDs nanocomposite were estimated by the following equation that was developed for predicting CdTe QD core diameters based on their absorbance properties [39]:

$$D = (9.8127 \times 10^{-7}) \times \lambda^3 - (1.7147 \times 10^{-3}) \times \lambda^2 + (1.0064) \times \lambda - 194.84$$

In the above equation, D is the theoretical diameter of the CdTe QD core and λ is the measured excitonic peak wavelength. Herein, λ was obtained by the excitonic peak

wavelength of Fig. 1b for each sample. The calculated particle sizes of the CdTe QD core were about 3.43, 3.44, 3.47, 3.50, and 3.51 when SA concentrations were 0, 0.05, 0.1, 0.15, and 0.3 g/mL, respectively. It was sure that the size of the SA/QDs nanocomposite was greater than the CdTe QD core as indicated in the TEM images. Because the highest fluorescence intensity was found for the SA/QDs nanocomposite with 0.1 g/mL of SA, the optimum amount of SA for the system was chosen to be about 0.1 g/mL.

To determine the ratio of SA and GSH-CdTe/ZnS QDs, the amount of GSH-CdTe/ZnS QDs was kept constant while the amount of SA was varied. As shown in Fig. 1c, with increasing ratio of SA:GSH-CdTe/ZnS QDs, the fluorescence intensity was increased until the ratio reached to 3:1. When over that ratio, the fluorescence intensity decreased gradually. Therefore, the best enhancing effect would be obtained when the ratio of SA:GSH-CdTe/ZnS QDs was about 3:1.

Fig. 1d shows the fluorescence intensity of the SA/QDs nanocomposite by changing the reaction temperature during synthesis. The fluorescence intensity clearly decreased when the reaction temperature increased from 25 °C to 100 °C. Similar results were reported that high temperature contributed to decomposition of the polymeric shell of QDs and thus a change in fluorescence intensity of dots [32].

The effect of aging on the fluorescence properties of the SA/QDs nanocomposite was also measured (Fig. 1e). The results showed that the fluorescence intensity of the SA/QDs nanocomposite did not change compared with GSH-CdTe/ZnS QDs. Therefore, the SA/QDs nanocomposite had good long-term stability, suggesting a role as a probe in biological systems imaging [5].

The optimization results showed that the high fluorescence intensity of the SA/QDs nanocomposite was obtained when the concentration of SA in solution was 0.1 g/mL, ratio of SA:GSH-CdTe/ZnS QDs was 5:1, and temperature of reaction was 25 °C. Therefore, we used this nanocomposite for further investigation throughout this manuscript.

Structure and composition characterization

FT-IR spectroscopy was employed to study the surface functional groups of SA/QDs nanocomposite. FT-IR spectra of SA, GSH-CdTe/ZnS QDs, and the SA/QDs nanocomposite are presented in Fig. 2a. In the FT-IR spectra of SA, absorption peaks of -OH and C = O groups at 3390 and 1614 cm^{-1} were observed, respectively. In the FT-IR spectra of GSH-CdTe/ZnS QDs, absorption peaks of -OH, C = O, and CdTe/ZnS groups at 3452, 1634, and 618 cm^{-1} were detected, respectively. In the FT-IR spectra of the SA/QDs nanocomposite, the all characteristic absorption peaks of SA and GSH-CdTe/ZnS QDs were found. However, the stretching vibration of the carbonyl (1634 cm^{-1}) and hydroxyl (3452 cm^{-1}) groups of SA was shifted to lower wavelengths (1603 cm^{-1} for carbonyl

and 3387 for hydroxyl) in the FT-IR spectrum of the SA/QDs nanocomposite. These differences indicate the chelating formation of SA biopolymer functional groups on the surface of GSH-CdTe/ZnS QDs. To investigate further, the FT-IR spectrum of the SA/QDs nanocomposite was compared with the FT-IR spectrum of GSH-CdTe/ZnS QDs. As can be seen from Fig. 2a, there are obvious differences among these spectra due to the formation of a polymeric shell around QDs.

Thermal stability of SA and SA/QDs nanocomposite were studied by TGA in the range 35–600 °C at a heating rate of 20 °C/min (Fig. 2b). Three successive weight loss steps were detected in both samples. The first gradual weight loss step was around 100 °C attributable to the removal of water molecules, signified as OH vibrations in FT-IR analysis. The second weight loss step was observed at around 235 °C for SA and 225 °C for the SA/QDs nanocomposite due to the degradation of the polymer chains. The third weight loss step occurred at around 345 °C for SA and 295 °C for the SA/QDs nanocomposite and was related to elimination of CO and CO₂ from samples. TGA profiles showed that the weight loss percentage of the SA/QDs nanocomposite at 600 °C is higher than that of pure SA. This was due to the additional GSH-CdTe/ZnS QDs in the SA biopolymer. According to DTA results, endothermic reactions cause the decomposition of the samples at these temperatures. The highest exothermic reaction was occurred at 258 °C for SA and 251 °C for SA/QDs nanocomposite.

Fig. 2c shows the typical TEM images of GSH-CdTe/ZnS QDs and SA/QDs nanocomposite. It can be seen that GSH-CdTe/ZnS QDs were dispersed into the SA biopolymer, and the density of QDs was not very high. The diameters of GSH-CdTe/ZnS QDs and SA/QDs nanocomposite were in the range of several nanometers (<7 nm) for both samples.

Fluorescence response of SA/QDs nanocomposite towards amantadine

Under the experimental conditions, the fluorescence spectra of the SA/QDs nanocomposite were investigated in the absence and presence of amantadine (Fig. 3). It was observed that a progressive decrease in the fluorescence intensity of the SA/QDs nanocomposite was caused by different concentrations of amantadine. The results proved that the quenching effect of the amantadine was concentration dependent.

Optimum reaction conditions between SA/QDs nanocomposite and amantadine

The influence of acidity on fluorescence intensity of the SA/QDs nanocomposite–amantadine solution was investigated (Fig. 4a). The results revealed that the maximum value of fluorescence intensity was obtained when the pH was 7.4.

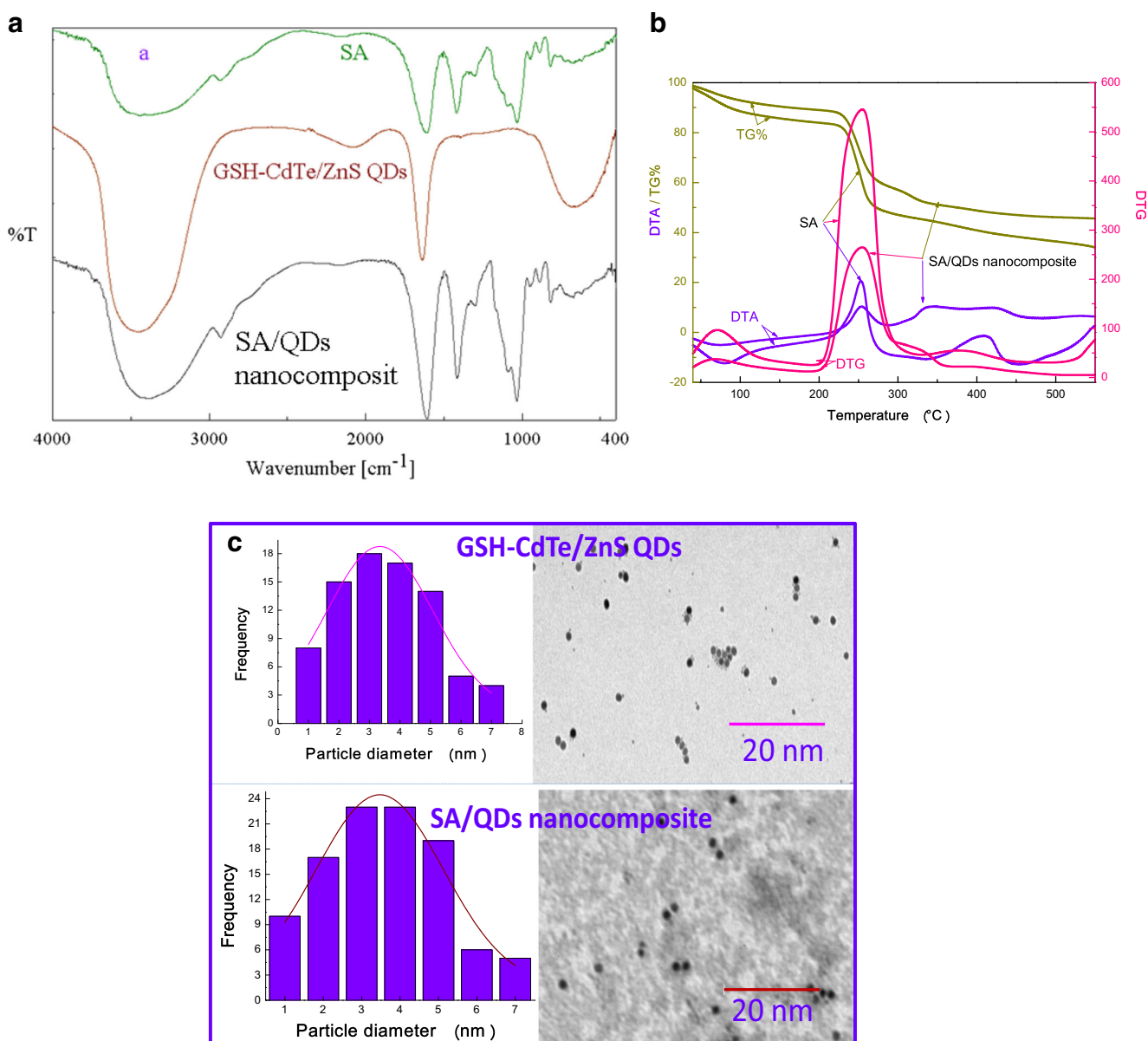


Fig. 2 (a) FT-IR spectra of SA, GSH-CdTe/ZnS QDs, and SA/QDs nanocomposite, (b) thermal stability of SA and SA/QDs nanocomposite, and (c) TEM images of GSH-CdTe/ZnS QDs and SA-GSH-CdTe/ZnS

As a result, pH 7.4 was chosen to be the optimal reaction pH in this experiment.

The effect of QDs concentration on the fluorescence intensity of the SA/QDs nanocomposite–amantadine solution was studied (Fig. 4b). The experiment results indicated that the SA/QDs nanocomposite concentration strongly influenced the fluorescence intensity of the SA/QDs nanocomposite–amantadine solution, and the optimum amount of SA/QDs nanocomposite was about 3.53×10^{-6} mol/L.

Fig. 4c shows the effect of incubation time on fluorescence intensity of the SA/QDs nanocomposite–amantadine solution. The results showed that a rapid decrease in fluorescence intensity of QDs occurred after addition of amantadine. The reaction was completed within 10 min at room temperature

and stable for over 110 min. Thus, a time scale of 10 min was selected as the detection time throughout this research.

Possible interaction mechanism

Fluorescence quenching can result from variety of molecular interactions including molecular rearrangements, fluorescence resonance energy transfer effect (FRET), electron transfer (ET), excited state reactions, complex formation, and collisional quenching [40, 41]. However, quenching mechanisms of fluorescence emission from QDs by non-fluorophore materials (such as amantadine) are usually divided into two categories, static quenching and dynamic quenching [23]. Static quenching results from the formation of a complex in the ground state, the

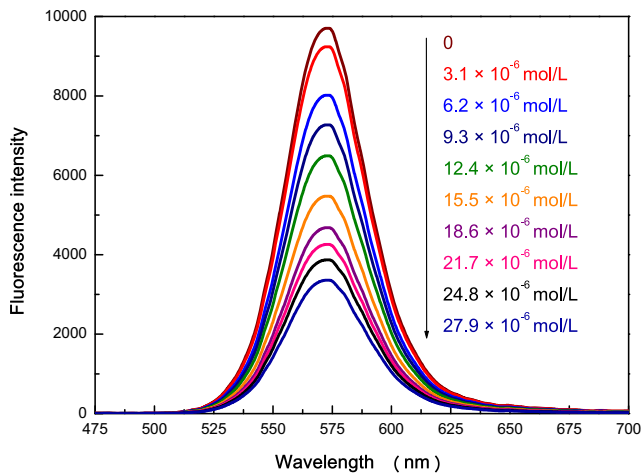


Fig. 3 Fluorescence spectra of the SA/QDs nanocomposite with different concentration of amantadine drug

same as before excitation occurs. The formed complex is non-fluorescent and has a unique absorption spectrum. Unlike static quenching, dynamic quenching occurs when the fluorophore return to the returns to the ground state without ant photochemical reactions. In order to distinguish dynamic or static quenching of QDs in the presence of amantadine, the Stern–Volmer equation was used as follows [25, 26]:

$$F_0/F = 1 + K_{SV}[Q]$$

where F_0 and F are the fluorescence intensity in the absence and presence of amantadine quencher, respectively. $[Q]$ is the molar concentration of the amantadine quencher, and K_{SV} is the Stern–Volmer constant. As shown in Fig. 5, there was a good linear relationship between the quenching effect of the

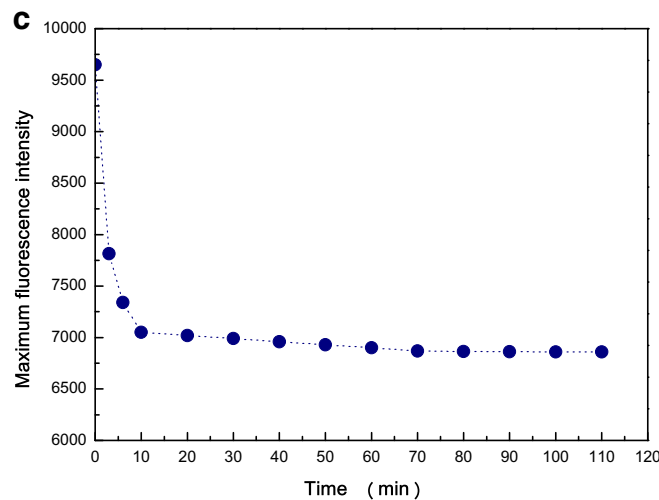
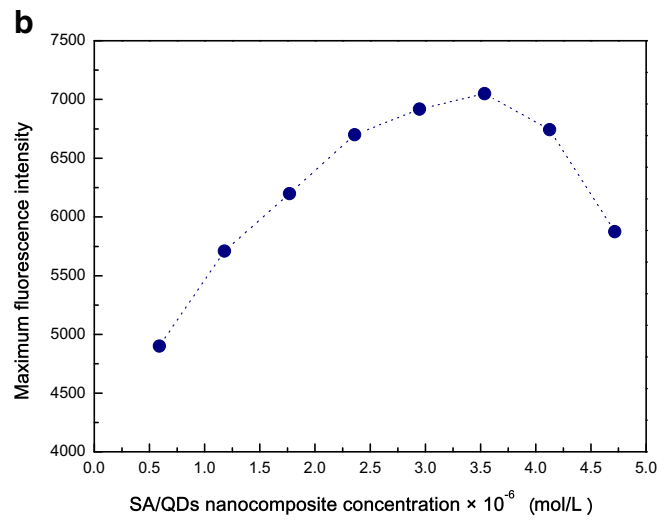
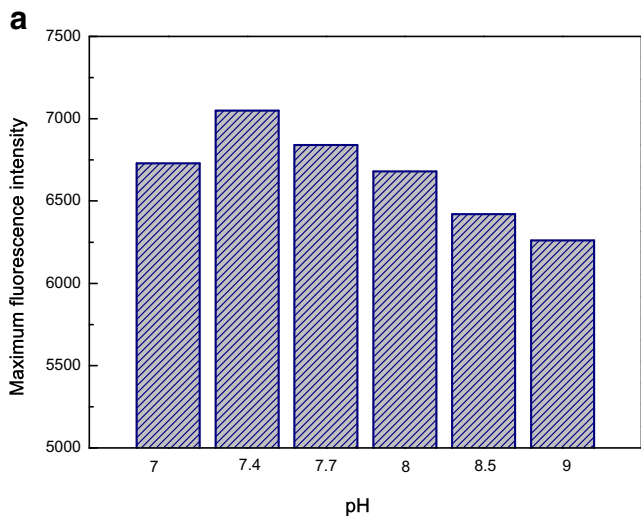


Fig. 4 (a) effect of pH ($C_{\text{amantadine}} = 9.3 \times 10^{-6}$ mol/L, $C_{\text{nanocomposite}} = 3.53 \times 10^{-6}$ mol/L, and $t_{\text{incubation}} = 10$ min), (b) SA/QDs nanocomposite concentration ($C_{\text{amantadine}} = 9.3 \times 10^{-6}$ mol/L, pH = 7.4, and $t_{\text{incubation}} = 10$ min), and (c) incubation time

($C_{\text{amantadine}} = 9.3 \times 10^{-6}$ mol/L, $C_{\text{nanocomposite}} = 3.53 \times 10^{-6}$ mol/L, and pH = 7.4) on the fluorescence intensity of the SA/QDs nanocomposite–amantadine solution at room temperature

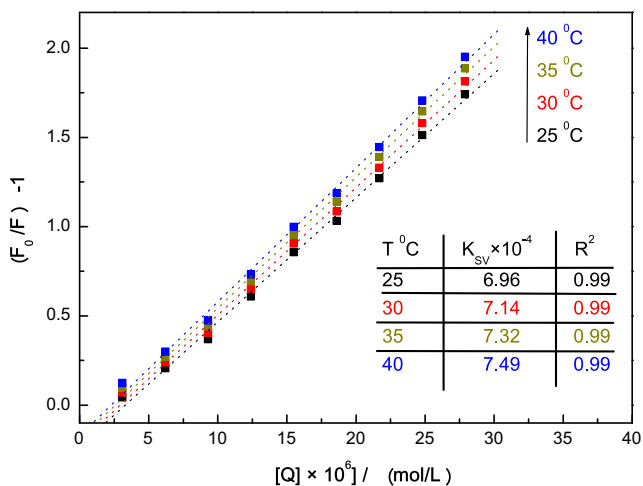


Fig. 5 Stern–Volmer plots for the optimized SA/QDs nanocomposite–amantadine solution at different temperatures

amantadine and the amantadine concentration over the concentration range of $3.1\text{--}27.9 \times 10^{-6}$ mol/L. Table in Fig. 5 listed the various values of K_{SV} at the 25, 30, 35, and 40 °C temperatures. As could be seen, the values of K_{SV} increased with the increasing temperature which indicates that the fluorescence quenching processes of QDs by amantadine was dynamic quenching processes. This was caused by faster diffusion, and hence a larger collision rate occurred at higher temperatures.

Standard curves

The fluorescence spectra of SA/QDs nanocomposite with different concentrations of amantadine were recorded under the optimum experimental conditions (Fig. 5) to estimate the quenching equation. The results showed that the best linear relationship between F_0/F and the concentration of GSH-CdTe/ZnS QDs [Q] was in the range of $3.1\text{--}27.9 \times 10^{-6}$ mol/L. The linear equation was $F_0/F = 0.0696Q - 0.229$ with

Table 1 Coexistent substances effect on the fluorescence emission of the of optimized SA/QDs nanocomposite–amantadine solution

Coexisting substances	Coexisting concentration (μg/mL)	Relative error (%)
l-tryptophan	60	+3.4
Phthalic acid	15	+2.8
Glycerol	800	+2.7
Glucose	840	+1.9
HSA	50	+5.1
K^+ (SO_4^{2-})	400	+0.1
Na^+ (Cl^-)	400	+1.2
Cu^{2+} (SO_4^{2-})	1.0	−0.8
Fe^{3+} (SO_4^{2-})	1.5	−1.3
Ca^{2+} (NO_3^-)	26	+0.7

correlation coefficients of 0.99. The detection limit was compute by the following equation:

$$\text{Detection limit} = t_{(n-1, 1-\alpha=0.99)} \times S_s$$

which $t_{(n-1, 1-\alpha=0.99)}$ is the Student's t-value appropriate for a single-tailed 99th percentile t statistic and a standard deviation estimate with n-1 degrees of freedom. S_s is sample standard deviation of the replicate spiked sample analyses. The detection limit was calculated about 0.9×10^{-6} mol/L at 25 °C.

Interference of co-existing foreign substances

A variety of co-existing foreign substances are present in the biological solution, which often interfere with the analysis. Therefore, a cleanup procedure is required before analysis. Herein, fluorescence emission response of the nanocomposite upon addition of some familiar foreign ions and excipients such as l-tryptophan, phthalic acid, glycerol, glucose, HSA, K^+ (SO_4^{2-}), Na^+ (Cl^-), Cu^{2+} (SO_4^{2-}), Fe^{3+} (SO_4^{2-}), and Ca^{2+} (NO_3^-) were examined at the same conditions. These materials are mostly contained in commercial capsules and pills. The same experiments with these materials are also reported in previous literatures due to possibility of practical application of their procedures. From Table 1, it was observed that most of the common metal ions and excipients did not produce any noticeable effect on the fluorescence emission of the QDs even at higher concentration. However, it was noteworthy from Table 1 that Fe^{3+} and Cu^{2+} quench the fluorescence of QDs. Thus, they could be allowed at lower concentration levels without significant interference. The same results were obtained in most of the nanoprobe based on QDs [21, 23, 30, 31].

Analytical application

To demonstrate that the proposed method was feasible, the fluorescent SA/QDs nanocomposite was applied to determine amantadine in commercial capsules. Moreover, to evaluate the accuracy of the developed method, the samples were analyzed with the reference HPLC method for the assay of amantadine. The results are shown in Table 2. It can be seen that the relative standard deviation (RSD) was lower than 2.3, which indicates that the proposed method is in good agreement with

Table 2 Result for amantadine determination in commercial capsules

Amantadine capsules samples	HPLC procedures (mg)	Our proposed procedures (mg)	RSD (%) ($n = 3$)
1	100.2	99.6	1.6
2	99.4	99.5	2.3
3	99.7	99.6	1.9

those using the HPLC method and can meet the requirement of microanalysis in the sample.

Conclusion

In this paper, we presented for the first time an uncomplicated route to prepare a novel simple fluorescence nanosensor for rapid sensing of amantadine. It was successfully constructed by embedding GSH capped CdTe/ZnS QDs into SA biopolymer. The obtained QDs were characterized using TEM, TGA, FT-IR, fluorescence, and UV–vis spectroscopy. The results showed that fluorescence intensity of GSH-CdTe/ZnS QDs was significantly improved after embedding into SA. The sizes of the prepared QDs were about ~3.5 nm. With the addition of amantadine, the fluorescence intensity of QDs decreased considerably. We optimized some important factors which would affect on the fluorescence intensity in the interaction between QDs and amantadine. Under the optimized experimental conditions, amantadine quenched the fluorescence intensity of QDs by dynamic mechanism. In addition, a linear calibration plot was observed for the fluorescence quenching at 576 nm against the amantadine concentration in the range of $3.1\text{--}27.9 \times 10^{-6}$ mol/L with a correlation coefficient of 0.99. The assay was satisfactory applied to the amantadine determination in real samples. We expect that the proposed sensor with high sensitivity, rapid response, low cost, and stability will be applied to improve performance of biosensors.

Acknowledgements We sincerely thank Payame Noor University, National Elites Foundation, and Iran Nanotechnology Initiative Council for funding this work.

References

1. Chauhan VM, Hopper RH, Ali SZ, King EM, Udrea F, Oxley CH, Aylott JW (2014) *Sens Actuators B Chem* 192:126
2. Vyas SS, Jadhav SV, Majee SB, Shastri JS, Patravale VB (2015) *Biosens Bioelectron* 70:254
3. Zhu X, Xiao Y, Jiang X, Li J, Qin H, Huang H, Zhang Y, He X, Wang K (2016) *Talanta* 151:68
4. Liu Z, Li G, Xia T, Su X (2015) *Sens Actuator B Chem* 220:1205
5. Yang P, Zhu B, Zhao J, Yu H, Yan L, Wei Q, Du B (2013) *Inorg Chim Acta* 408:120
6. He L, Li J, Xin JH (2015) *Biosens Bioelectron* 70:69
7. Qian ZS, Shan XY, Chai LJ, Chen JR, Feng H (2015) *Biosens Bioelectron* 68:225
8. Hu K, Huang Y, Wang S, Zhao S (2014) *J Pharm Biomed* 95:164
9. Tian J, Liu Q, Asiri AM, Sun X, He Y (2015) *Sens Actuators B Chem* 216:453
10. Liu S, Wang L, Luo Y, Tian J, Li H, Sun X (2011) *Nano* 3:967
11. Hansda C, Chakraborty U, Hussain SA, Bhattacharjee D, Paul PK (2016) *Spectrochim Acta A* 157:79
12. Rong M, Lin L, Song X, Wang Y, Zhong Y, Yan J, Feng Y, Zeng X, Chen X (2015) *Biosens Bioelectron* 68:210
13. Mansur HS (2010) *Wiley Interdiscip Rev Nanomed Nanobiotechnol* 2:113
14. Badawi A (2015) *J Mater Sci-Mater El* 26:3450
15. Sung T, Lo Y, Chang I (2014) *Sens Actuators B Chem* 202:1349
16. Ananth DA, Rameshkumar A, Jeyadevi R, Jagadeeswari S, Nagarajan N (2015) *Spectrochim Acta A* 138:684
17. Wang Y, Liu Y, He X, Li W, Zhang Y (2012) *Talanta* 99:69
18. Akshya S, Hariharan PS, Kumar VV, Anthony SP (2015) *Spectrochim Acta A* 135:335
19. Wang A, Fu L, Rao T, Cai W, Yuen M, Zhong J (2015) *Opt Mater* 42:548
20. Chakravarty S, Dutta P, Kalita S, Sarma NS (2016) *Sens Actuators B Chem* 232:243
21. Yu Y, Xu L, Chen J, Gao H, Wang S, Fang J, Xu S (2012) *Colloids Surface B* 95:247
22. Shen Y, Liu S, Yang J, Wang L, Tan X, He Y (2014) *Sens Actuators B Chem* 199:389
23. Ying S, Cui S, Wang W, Feng J, Chen J (2014) *J Lumin* 145:575
24. Lima AS, Rodrigues SSM, Korn MGA, Ribeiro DSM, Santos JLM (2014) *Microchem J* 117:144
25. Wang X, Lv Y, Hou X (2011) *Talanta* 84:382
26. Ensafi AA, Kazemifard N, Rezaei B (2015) *Biosens Bioelectron* 71:243
27. Liu Y, Yu J (2010) *J Colloid Interf Sci* 351:1
28. Adegoke O, Nyokong T (2013) *J Photochem Photobiol A* 265:58
29. Sekhosana KE, Antunes E, Khene S, D'Souza S, Nyokong T (2013) *J Lumin* 136:255
30. Liu Z, Yin P, Gong H, Li P, Wang X, He Y (2012) *J Lumin* 132:2484
31. Adegoke O, Nyokong T (2013) *J Lumin* 134:448
32. Bardajee GR, Hooshyar Z (2016) *Mat Sci Eng C* 62:806
33. Bardajee GR, Hooshyar Z, Mizani F (2014) *Mat Sci Semicon Proc* 19:89
34. Bardajee GR, Hooshyar Z (2013) *Spectrochim. Acta A* 114:622–626
35. Bardajee GR, Hooshyar Z, Jafarpour F (2013) *J Photochem Photobiol A* 252:46
36. Bardajee GR, Hooshyar Z, Rezanezhad H, Guerin G (2012) *ACS Appl Mater Interfaces* 4:3517
37. Dekamin MG, Peyman SZ, Karimi Z, Javanshir S, Naimi-Jamal MR, Barikani M (2016) *Int J Biol Macromol* 87:172
38. Bhutani U, Laha A, Mitra K, Majumdar S (2016) *Mater Lett* 164:76
39. Yu WW, Qu L, Guo W, Peng X (2003) *Chem Mater* 15:2854
40. Sha J, Tong C, Zhang H, Feng L, Liu B, Lü C (2015) *Dyes Pigments* 113:102
41. Liu B, Tong C, Feng L, Wang C, He Y, Lü C (2014) *Chem Eur J* 20:2132